OPTICAL METHOD OF INVESTIGATION OF HEAT-TRANSFER MECHANISM IN BUBBLED BOILING

V. I. Baranenko and G. F. Smirnov

UDC 536.423.1:532.526

The results of an experimental investigation of the heat-transfer mechanism in boiling water with the use of a diffraction laser interferometer are presented in this article. It is shown that the analysis of the interferograms enables one to obtain local quantitative characteristics of the process and determine the scale of the temperature fluctuations in the zone of action of the center of vapor formation.

In [1-3] optical methods were used for the study of the boiling heat-transfer mechanism. However, the results obtained in these works are mainly of a qualitative nature.

A diffraction interferometer which permits quantitative as well as qualitative study of the processes occurring in the thermal boundary layer during boiling is described in [4].

The results of an investigation of the temperature profiles in the thermal boundary layer are discussed in [5, 6]. It is shown that from the interferograms of the thermal boundary layer it is possible to compute local temperature distributions and, hence, local thermal loads, with an accuracy up to 20%.

The results of an experimental investigation of the heat-transfer mechanism during bubbled boiling of water with underheating in the free volume under atmospheric-pressure conditions are given below. The experiments were conducted with the use of photographic and cinematographic pictures on the experimental equipment described in [4]. The photographs were taken with an enlargement of 3-4 by a Zenith-3M camera; the cinematographic pictures were taken in the natural scale by a high-speed motion-picture camera SKS-1. Because of the large enlargement scale, the photographs produced clearer interferograms than the cinematographic pictures. Therefore, interferograms obtained with the photographic camera were used for the quantitative analysis. The heater elements were prepared from wires with 0.07-0.4 mm diameter or thin strips with 0.7-1.5 mm width and thickness of a few hundredths of a millimeter. In a number of experiments the strips were fixed to a glass textolite base. The heaters were made of platinum or nickel.

Motion pictures of the process of bubbled boiling of water with underheating by a platinum wire of 0.15 mm diameter are shown in Fig. 1. The pictures were taken at a rate of 7700 frames per second, the thermal flux was $q_1 = 0.39 \cdot 10^6$ W/m^2, the temperature of the wall 130°C, and the temperature of the liquid 80°C. The bright background on the frames is the thermal boundary layer. The dark lines in the thermal boundary layer are the interference bands. The operation of two centers of vapor formation was recorded on the motion-picture photographs. The left center appears in the form of a jet of overheated liquid. The phases of growth, collapse, and condensation of the bubble are absent for this center of vapor formation. The appearance of the bubble in the right center is recorded on the second frame. The bubble grows in

TABLE 1

	1	2	3	4	5	6			
	$d_M \cdot 10^3$, m	$\tau_* \cdot 10^3$, sec	$\tau_p \cdot 10^3$, sec	$\tau_0 \cdot 10^3$, sec	No.	d_M, %	τ_*, %	τ_p, %	τ_0, %
Left	0.75	1.26	0.3	8.6	46	4	2	3	0.3
Right	1.7	5.4	0.3	68	8	10	4	6	4

Nikolaev—Odessa. Translated from Zhurnal Prikladnoi Mekhanika i Tekhnicheskoi Fiziki, No. 1, pp. 170-176, January-February, 1973. Original article submitted April 17, 1972.

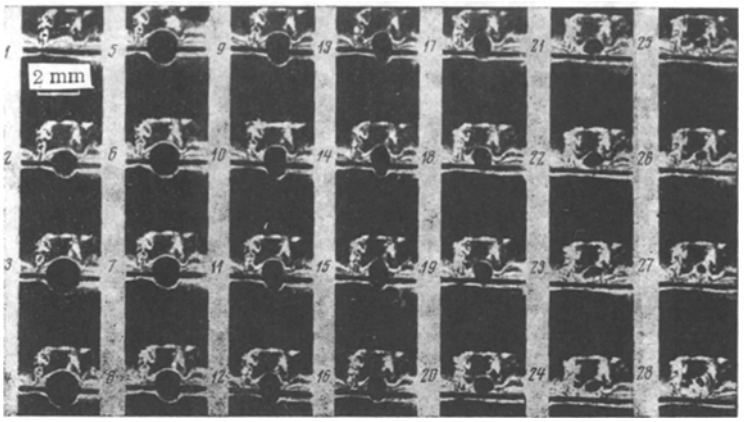

Fig. 1

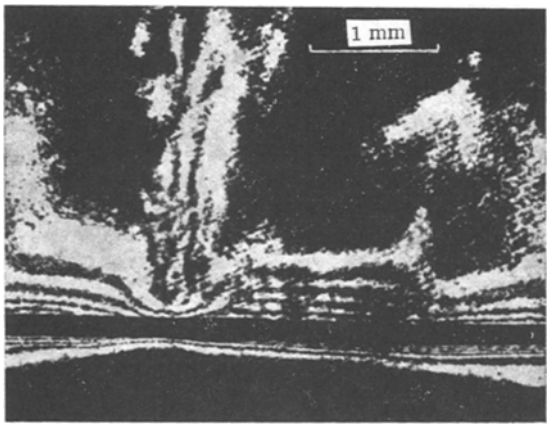

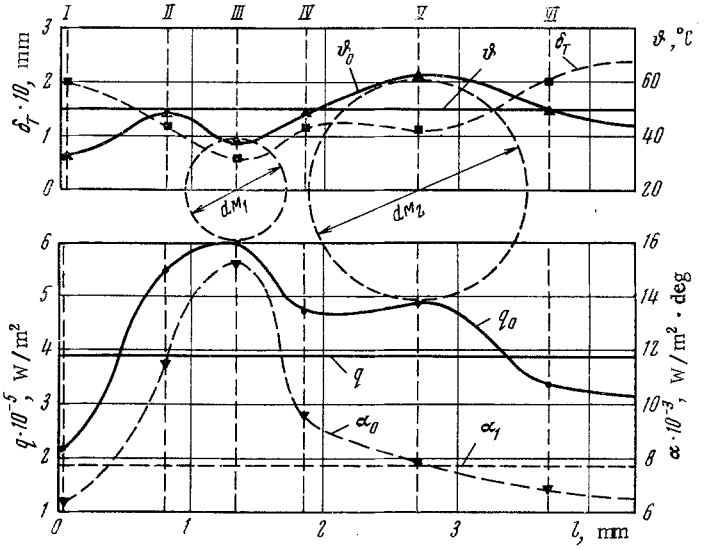

Fig. 2

frames 2-4, the condensation up to the instant of collapse occurs in frames 5-21, and the condensation after the collapse occurs in frames 22-28.

An inspection of all motion-picture frames (about 5000 frames) made it possible to establish the following.

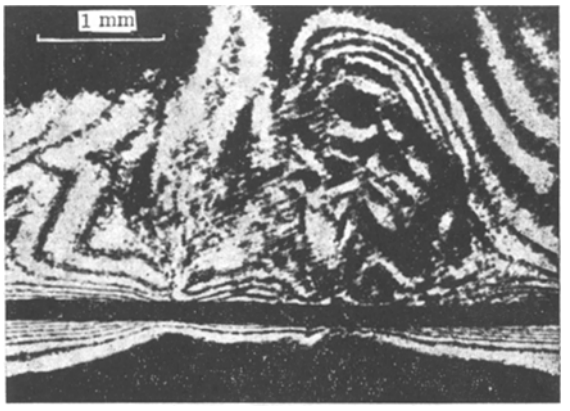

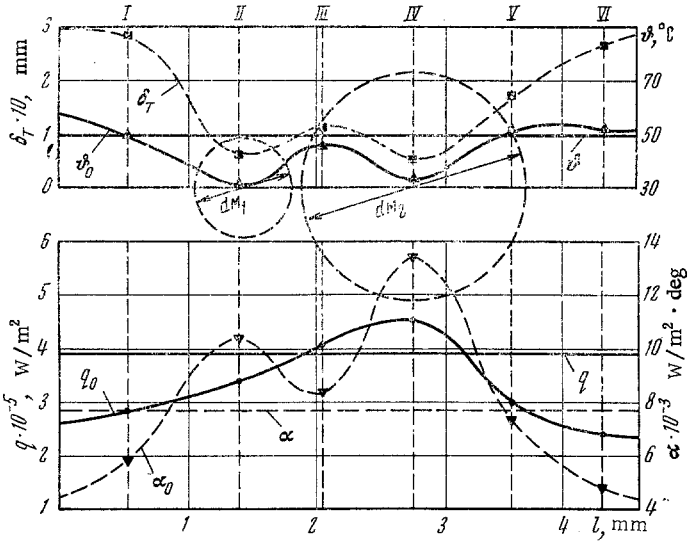

Fig. 3

1. The nature of the process in each operating center of vapor formation is reproduced within a single regime. The results of the analysis are given in Table 1. It is seen from the table that the root-mean-square error of determination of the main characteristics of the operating centers of vapor formation does not exceed 10%. In Table 1, column 1 shows the maximum diameter d_m; 2 the life time, i.e., the time from the instant of formation of the bubble to the instant of collapse; 3 the growth time, i.e., the time in which the bubble attains its maximum size; 4, the melting period, i.e., the time from the collapse of the preceding bubble to the formation of the next; 5 the number of bubbles analyzed; 6 the root-mean-square error. In the determination of the life time it is not possible to measure the time up to complete condensation, since the scale of enlargement does not allow this. Therefore, the measured life time is the time of growth and condensation of the bubble to sizes 0.1-0.2 of the maximum.

2. During the waiting period jets of overheated liquid exist at the place of operation of the vapor-formation centers in a stable way; these are formed as a result of rupture and condensation of the bubbles. Since the time of dispersal of the jet is larger than the waiting time, on the motion-picture frames the jets of overheated liquid are recorded as continuous.

3. The condensation of the bubble starts from its lateral surfaces adjoining the heater. The rupture diameter of the bubble is smaller than the maximum. The shape of the bubble is close to a sphere at the time of growth and departs from it during condensation.

4. The appearance of bubbles leads to a change of the structure of the thermal boundary layer. During the waiting period the thermal boundary layer gets restored; during the growth and condensation of the bubble it disintegrates.

Interferograms taken in the same regime as for the motion pictures of Fig. 1 are shown in Figs. 2 and 3. Figure 2a shows the interferogram of frame No. 1 in Fig. 1. The distribution of the local thermal

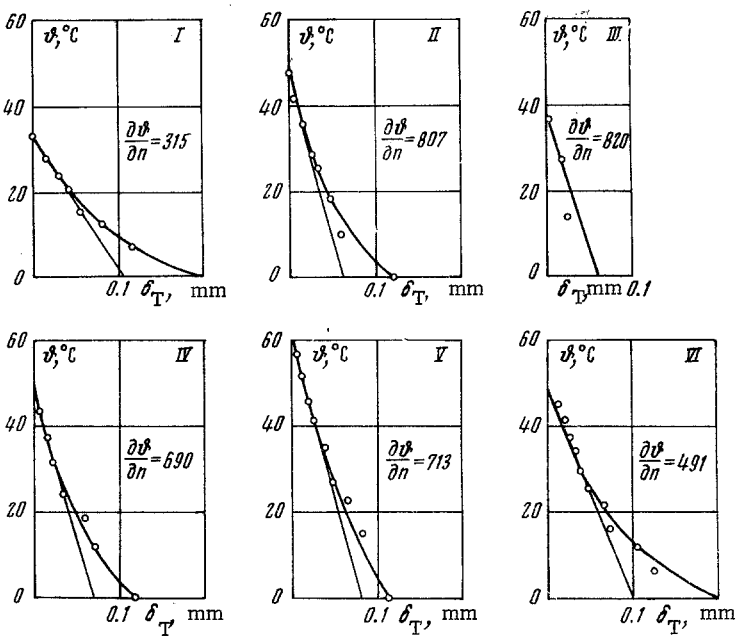

Fig. 4

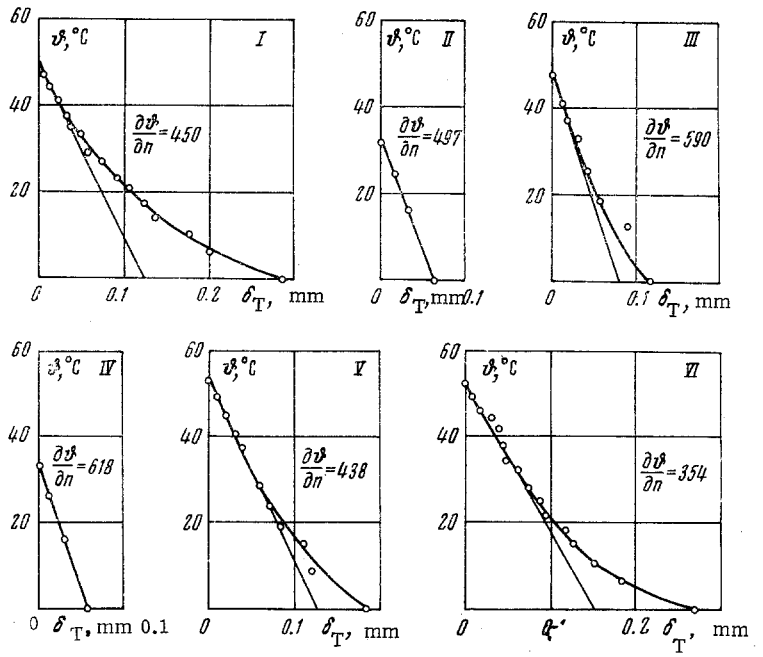

Fig. 5

fluxes q_0, the temperature thrusts ϑ_0, the heat-transfer coefficients α_0, and the thicknesses of the thermal boundary layer δ_T, at the lower forming wire are shown in Fig. 2b. Figure 3a shows the interferogram of boiling water with underheating corresponding to frame No. 28 of Fig. 1. The distribution of local thermal fluxes q_0, temperature thrusts ϑ_0, heat-transfer coefficients α_0, and thicknesses of the boundary layer δ_T for the photograph of Fig. 3a are shown in Fig. 3b. Since the exposure time for the photographs is larger than for the motion pictures, the interferogram in Figs. 2 and 3 correspond to 33 frames of the motion pictures shown in Fig. 1. Therefore, steam bubbles are not recorded on the interferograms. The interferogram of Fig. 2 corresponds roughly to the first and earlier frames, while the interferogram of Fig. 3 corresponds to the last and later frames.

The local values of the thickness of the thermal boundary layer from the side of the lower forming heater, the temperature thrust, the specific thermal flux, and the heat-transfer coefficient are shown below

the interferograms. The thickness of the thermal boundary layer was determined as the distance from the lower forming heater to the edge of the last bright interference band. The temperature thrust, the specific heat flux, and the heat-transfer coefficient were obtained by scaling of the interferogram from the side of the lower forming heater.

The interferograms permit the determination of the field of the refractive index in the thermal boundary layer. The transition from the refractive index field to the temperature field is accomplished with the use of the well-known Lorentz–Lorentz formula. The procedure of scaling of the interferograms is given in [4]. The temperature profiles in the thermal boundary layer were obtained from these computations. The profiles corresponding to the interferogram of Fig. 2 are shown in Fig. 4 and those corresponding to the interferogram of Fig. 3 are shown in Fig. 5.

The local temperature thrust is determined as the difference between the temperature of the liquid layer at the first interference band from the heater and the temperature of the liquid in the main volume. The local specific heat flux was found by graphical differentiation of the temperature profiles with the use of Fourier equation

$$q_0 = -\lambda \frac{\partial \vartheta}{\partial n} \tag{1}$$

where q_0 is the local specific heat flux, λ is the coefficient of thermal conductivity of the liquid, and $\partial\vartheta/\partial n$ is the temperature gradient near the heater. The values of the temperature gradient in deg/mm are shown in Figs. 4 and 5 for different sections along the length of the heater. The number of the sections is denoted by Roman numerals and is shown in Figs. 2 and 3; the linear scale of the graphs corresponds with the scale of the corresponding photograph. The local heat-transfer coefficient is determined as the ratio of the local heat flux to the corresponding temperature drop

$$\alpha_0 = \frac{q_0}{t_0 - t_*} = \frac{q_0}{\vartheta_0} \tag{2}$$

where t_0 is the local temperature of the heater computed from the interferogram, t_* is the temperature of the liquid in the main volume, and α_0 is the local heat-transfer coefficient. The local temperature of the heater was taken equal to the temperature of the first interference band from the heater.

An analysis of the local heat-transfer characteristics shown in Figs. 2-5 permits the following conclusions:

1. The thickness of the thermal boundary layer, the local temperature thrust, the specific heat flux, and the heat-transfer coefficient vary within wide ranges along the length of the heater. Thus, from the data of Figs. 2 and 3 the thickness of the thermal boundary layer changes by a factor of 5.3, the temperature thrust by a factor of 2, the specific heat flux by a factor of 3, and the heat-transfer coefficient by a factor of 2.6 over a 4-mm length of the heater.

2. The most intense heat transfer is obtained at the places of operation of the vapor-formation centers. The zone of operation of the center is equal to 1-1.5 of the maximum diameter of the bubble. In Figs. 2 and 3 the maximum diameters of the bubbles are shown by dashed circles.

3. The temperature profile is close to linear at the places of operation of the vapor-formation centers.

4. The thermal boundary layer is restored to a large extent at those centers where bubbles with large diameters, and hence with large waiting periods, are formed.

The average values of the heat-transfer characteristics obtained from electrical measurements are shown in Figs. 2 and 3 by dashed and continuous straight lines. It is evident from the figures that the local heat-transfer characteristics agree with the average values.

Motion pictures and photographs taken during boiling of water at wires of different diameters and plates give the same qualitative picture. The increase of underheating to the saturation temperature leads to a decrease of the diameters of the bubbles and their life time. However, even in this case hot jets of liquid are formed at the place of operation of the vapor-formation centers. On a plate the bubbles are close to a hemisphere in their shape at the growth stage. Interferograms obtained during boiling at plates are more complicated to decipher than those obtained during boiling at wires. For plates with 0.7-1.5 mm width the main difficulty in the interpretation involves the determination of the geometrical length of the path of the light ray in the thermal boundary layer.

LITERATURE CITED

1. N. Isshiki and H. Tamaki, "Photographic study of boiling heat-transfer mechanism," Bulletin JSME, 6, No. 23, 505 (1963).
2. Jacobs and Sheid, "Measurement of temperature in the process of bubble formation during boiling in a large volume, heat transfer," Am. Soc. Mech. Engrs., No. 2 (1969).
3. M. Bikhar, M. Kurto, R. Rik, and R. Semeri, "Main problems in the process of boiling of liquid underheated to saturation temperature in the presence and absence of dissolved gases," in: Advances in the Field of Heat Transfer [Russian translation], Mir, Moscow (1970).
4. V. M. Baranenko and Yu. D. Kardashev, "Problem of use of optical method for investigation of heat transfer during boiling," Tr. Nikolaev. Korablestroit. In-ta, No. 33 (1970).
5. V. I. Baranenko, "Experimental investigation of thermal boundary layer on thin cylindrical heater during natural convection in water," Tr. Nikolaev. Korablestroit. In-ta, No. 37, (1970).
6. G. F. Smirnov and V. I. Baranenko, "Experimental investigation of temperature profiles in thermal boundary layer during boiling of liquid in free volume," Inzh.-Fiz. Zh., 21, No. 2 (1970).